# A SEARCH FOR X-RAY REIONIZATION SIGNATURES FROM CROSS-CORRELATION OF *WMAP* AND ROSAT RASS DATA

Quan Guo[1,2], Xiang-Ping Wu[1], HaiGuang Xu[3] and JunHua Gu[3]

## ABSTRACT

We present an observational search for the possible correlation between cosmic microwave background (CMB) polarization map and soft X-ray background (SXRB) based on the ROSAT All-sky Survey (RASS) archive and WMAP five-year observations. This is motivated by the fact that some of the CMB polarization may arise from the scattering of CMB photons due to the free electrons generated by X-ray heating sources in the epoch of reionization. Detection of such a correlation allows one to study the role of X-ray heating in the process of reionization. However, the cross angular power spectrum of the CMB polarization and SXRB maps constructed from ROSAT RASS and WMAP five-year maps is consistent with no correlation. We attribute this negative detection to both the extremely weak signals and large instrumental noises. While a future search is needed with high sensitivity instruments for both CMB polarization and soft X-ray photons, our current results can still be used as a useful constraint on the effect of X-ray heating in the epoch of reionization.

*Subject headings:* cosmology: cosmic microwave background — large-scale structure — X-rays: galaxies

## 1. Introduction

Many efforts have been made so far to search for the correlation between cosmic microwave background (CMB) and X-ray sky, in an attempt to detect the signatures of both the integrated Sachs-Wolfe effect resulting from time-evolving potentials of large-scale

[1]National Astronomical Observatories, Chinese Academy of Sciences, Beijing 100012, China

[2]Graduate School of Chinese Academy of Sciences, Beijing 100049, China

[3]Department of Physics, Shanghai Jiao Tong University, 800 Dongchuan Road, Shanghai 200240, RPC

structures at late times, which can be traced by various X-ray sources, and the Sunyaev-Zel'dovich (SZ) effect due to the scattering of CMB photons by the ionized electrons in clusters of galaxies. Yet, no significant detections of the correlation signals have been reported using the ROSAT RASS data (Kneissl et al. 1997; Diego et al. 2003), in contrast to the positive results revealed by tracers of large-scale structures, including the hard (2-10 keV) X-ray background (Boughn & Jahoda 1993; Bennet et al. 1993; Banday et al. 1996) and galaxies observed in the radio, optical and infrared bands (e.g. Scranton et al. 2003; Boughn & Crittenden 2004a,b; Nolta et al. 2004; Myers et al. 2004; Fosalba & Gaztanaga 2004; Afshordi, Loh,&Strauss 2004; Pietrobon et al. 2006). In addition to the CMB-X-ray source correlation generated at late times, CMB polarization map may also correlate with the unresolved soft X-ray background (SXRB) presumably originated from supernovae, X-ray binaries and quasars at high-redshift beyond $z = 6$. These sources are believed to play a significant role in the heating of neutral gas through photoionization at the epoch of reionization (Dijkstra et al. 2004; Chen & Miralda-Escudé 2004), while the ionized electrons generate the CMB polarization signals, depending on both electron scattering optical depth and primordial quadrupole of CMB. Doré et al. (2007) note that such polarization signals on small scales are on order of 0.01 $\mu$K (see also Liu et al. 2001, for theoretical prediction) . But as of today a quantitative estimate of the correlation signals is still unavailable in the literature, and any of such detections will challenge the existing instrumental limits. The goal of this study is to make the first attempt at searching for such a correlation, using the current upper limits of the resolved diffuse SXRB and the recent WMAP polarization map.

A considerably large fraction ($\sim 94\%$, see Moretti et al. 2003) of soft and hard X-ray backgrounds have been resolved into discrete sources, and the maximum admitted ranges of the unresolved flux at different energy bands have been summarized in Wu & Xue (2001). If internal physical processes are properly treated, diffuse emission of hot gas in groups and clusters should also account for the residual SXRB after the removal off the discrete sources (Xue & Wu 2003). This indeed restricts the room for the presence of significant X-ray emission from high-redshift sources at the epoch of reionization (but see Salvaterra et al. 2007). So the fraction of soft X-ray which is emitted from high-redshift sources at the epoch of reionization could be not more than 5%. Furthermore, even if the correlation is detected, the signature may have been interlaced with those caused by the SZ effect, in the sense that the CMB polarization anisotropies may also be generated by hot electrons in clusters and even groups of galaxies (Shimon et al. 2006), unless foreground clusters and groups including distant ones can be masked in the search. In particular, the fluctuations of SXRB in the epoch of reionziation may appear at smaller scales comparable to or smaller than the sizes of clusters, because X-ray photons usually have relatively long free paths. This adds to further difficulties of our search for the signatures of X-ray reionization. Keeping these disadvantages

in mind, we perform an analysis of the correlation between the WMAP five-year polarization map and ROSAT RASS archive at energy band 0.2-2 keV, in the hope that current limits are helpful for placing robust constraints on models of X-ray reionization and for guiding future works on this topic.

## 2. Data

For WMAP five-year maps, we choose to work with the V and W bands in order to reduce foreground contamination. Furthermore, we restrict the analysis to the differently assembly polarization data denoted by V1, V2, W1, W2, W3, and W4, which are called WP sky maps hereafter. Full five-year sky maps are obtained by performing a weighted, pixel-by-pixel, mean of the single-year maps. Polarization signals are characterized by the Stokes parameter Q, U, and V. Because Thomson scattering can not generate circular polarization, we have $V = 0$. WMAP observes the sky with two orthogonal linear polarization modes per feed, which are sensitive to the Stokes parameter I, Q, and U (Hinshaw et al. 2007). These data were released in HEALPix[1] format with different resolutions. The map used in this work is of Res 9 ( $N_{\rm side} = 512$, which means the angular resolution is 6.87' ).

The ROSAT RASS (Snowden et al. 1997) covers the soft X-ray energy band ranging from 0.1 to 2 keV. The X-ray sky in lower energies is severely contaminated by local emission (Śliwa et al. 2001) while the X-ray sky in high energies shows a significant contribution from extragalactic AGNs. The RASS intensity ($I_{\rm SXRB}$) and noise ($\sigma$) maps are constructed by $I_{\rm SXRB} = (C - B)/t_{\rm exp}$ and $\sigma = \sqrt{C + B}/t_{\rm exp}$, respectively, where $C$ is the photon counts, $t_{\rm exp}$ is the exposure time and $B$ denotes the contamination, which comprises sources, particle background, scattered solar X-rays, long-term enhancements, and so on.

We use two types of SXRB maps constructed from different algorithms. The first one (hereafter RSI) is presented by Snowden et al. (1997). RSI covers approximately 98% of the sky in 1/4 keV, 3/4 keV, and 1.5 keV bands, each of which is further divided into two bands (R1+R2, R4+R5, R6+R7, respectively) with an angular resolution of about 12'. These maps were constructed using an equal-area polar projection and divided into six areas according to the six different projection pivots, in which the contamination sources, such as the particle background , scattered solar X-rays, and long-term enhancement, are excluded.

To produce an SXRB map with the angular resolution compatible to that of WMAP data, we construct the SXRB map (hereafter RSII map) in HEALPix format with Res 9

[1]See http://healpix.jpl.nasa.gov

($N_{\rm side} = 512$) from RASS archive with energy band ranging from 0.2 to 2 keV, in which each pixel covers an area of $6.87' \times 6.87'$ in the sky. Except for the correction to exposure time, we make no attempt to remove the bright point and diffuse sources from the local universe in order to optimize the detection of cross-correlation with the WMAP polarization maps, even if it has a local origin.

## 3. Statistical Method and Systematic Effects

Following Kogut et al. (2007), we expand the polarization fluctuations into generalized spherical harmonics

$$P^{(*)}(\mathbf{n}) = Q(\mathbf{n}) \pm iU(\mathbf{n}) = \sum a_{\mp,\ell m}\, {}_{\mp 2}Y_{\ell m}(\mathbf{n}). \tag{1}$$

The polarization fluctuations are conventionally decomposed into E- and B-modes. Introducing a weighting function $w^P(\mathbf{n})$, we can write the E-mode as

$$\begin{aligned} \widetilde{a}^E_{\ell m} &= \frac{1}{2}\int d\mathbf{n} w^P(\mathbf{n})[Q(\mathbf{n})({}_2Y^*_{\ell m}(\mathbf{n}) +_{-2} Y^*_{\ell m}(\mathbf{n})) \\ &\quad -iU(\mathbf{n})({}_2Y^*_{\ell m}(\mathbf{n}) -_{-2} Y^*_{\ell m}(\mathbf{n}))], \end{aligned} \tag{2}$$

and its angular power spectrum is given by

$$C^E_\ell = \frac{1}{2\ell+1}\sum_{m=-\ell}^{\ell} a^E_{\ell m} a^{*E}_{\ell m}. \tag{3}$$

The fluctuation of SXRB intensity $\Delta I$ can be decomposed in spherical harmonics as well

$$\Delta I(\mathbf{n}) = \sum_{\ell=0}^{\infty}\sum_{m=-\ell}^{l} a_{\ell m} Y_{\ell m}(\mathbf{n}), \tag{4}$$

and the corresponding angular power spectrum is

$$C^I_\ell = \frac{1}{2\ell+1}\sum_{m=-\ell}^{\ell} a^I_{\ell m} a^{*I}_{\ell m}. \tag{5}$$

We define the cross-correlation power spectrum between CMB E-mode map and SXRB as

$$C^x_\ell = \frac{1}{2\ell+1}\sum_{m=-\ell}^{\ell} a^E_{\ell m} a^{*I}_{\ell m}. \tag{6}$$

To construct the angular power spectrum from the observations, masks are often employed to account for the incomplete or inhomogeneous sky coverages, or excisions of contaminated regions, which are all incorporated in a window function $W(\mathbf{n})$. For the WMAP polarization map, we choose the window function $W_p(\mathbf{n})$ from the WMAP prescription (Bennett et al. 2003), and we apply the natural weighting assumption to the window function for the ROSAT map, namely $W_I(\mathbf{n}) = 0$ in the excised regions and $W_I(\mathbf{n}) = 1$ elsewhere. The cross-power spectrum between SXRB and WMAP polarization maps $C_l^x$ in the presence of incomplete sky coverage is modified by

$$\widetilde{C}_\ell^x = \frac{1}{2\ell+1}\sum_m \widetilde{I}_{\ell m}\widetilde{E}^*_{\ell m} \tag{7}$$

Such a pseudo cross-power spectrum $\widetilde{C}_l^x$ can be related to the unbiased whole sky power spectrum through their ensemble averages in terms of the algorithm MASTER (Hivon et al. 2002; Hansen & Górski 2003; Challinor & Chon 2005; Brown et al. 2005).

$$\langle\widetilde{C}_\ell^x\rangle = \sum_{\ell'} M_{\ell\ell'}\langle C_{\ell'}^x\rangle, \tag{8}$$

where $M_{ll'}$ describes the mode-mode coupling

$$M_{\ell\ell'} = \frac{(2\ell'+1)}{4\pi}\sum_{\ell''}\mathcal{W}_{\ell''}^{IP}\begin{pmatrix}\ell & \ell' & \ell''\\ 0 & 0 & 0\end{pmatrix}\begin{pmatrix}\ell & \ell' & \ell''\\ 2 & -2 & 0\end{pmatrix}, \tag{9}$$

and $\mathcal{W}^{IP}$ is the cross-power spectrum of the window functions

$$\mathcal{W}_\ell^{IP} = \sum_m w_{\ell m}^I (w_{\ell m}^P)^*, \tag{10}$$

with $w_{\ell m}^I$ and $w_{\ell m}^P$ defined as the spherical harmonic coefficients.

The angular power spectrum $\widetilde{C}_\ell^x$ should be further corrected for the smoothing effects of both instrumental beams ($B$), finite pixels ($p$) and noise ($N$)

$$\langle\widetilde{C}_\ell^x\rangle = \sum_{\ell'} M_{\ell\ell'}B_{\ell'}^I B_{\ell'}^P p_{\ell'}^I p_{\ell'}^P\langle C_{\ell'}\rangle + \langle\widetilde{N}\rangle \tag{11}$$

where $B_{\ell'}^I$ and $B_{\ell'}^P$ are the Fourier transforms of beam patterns of ROSAT and WMAP, respectively. The pixel window function in Eq. (11) is defined by

$$p_\ell = \left(\frac{1}{N_{\rm pix}}\sum_{i=0}^{N_{\rm pix}-1}|p_\ell(i)|^2\right)^{1/2}, \tag{12}$$

and the $m$-averaged window function reads

$$p_\ell(i) = \left( \frac{4\pi}{2\ell+1} \sum_{m=-\ell}^{\ell} |p_{\ell m}(i)|^2 \right)^{1/2}, \tag{13}$$

in which $p_{\ell m}$ is the spherical harmonic transform of pixel function $P_{\rm pix}(\mathbf{n}) = 1/\Omega_{\rm pix}$, and $\Omega_{\rm pix}$ is the solid angle subtended by one pixel.

Finally, the angular power spectrum should be properly binned to reduce the systematic effects described above, and the associated errors should also be estimated. With the algorithms MASTER and its extension to polarization, we can convert $\langle \widetilde{C}_\ell^x \rangle$ to an 'unbiased' whole sky angular power spectrum $\widehat{\mathcal{C}}$ and evaluate the errors of $\widehat{\mathcal{C}}$. In order to calculate the errors and covariance of the $\widehat{\mathcal{C}}$, we produce a number of mock observational maps by Monte Carlo simulations. So the elements of the covariance matrixes are given by

$$\mathrm{C_{bb'}} = \left\langle \left( \widehat{\mathcal{C}}_{\rm b} - \langle \widehat{\mathcal{C}}_{\rm b} \rangle_{\rm MC} \right) \left( \widehat{\mathcal{C}}_{\rm b'} - \langle \widehat{\mathcal{C}}_{\rm b'} \rangle_{\rm MC} \right) \right\rangle_{\rm MC}. \tag{14}$$

The error bars on $\widehat{\mathcal{C}}_b$ are then given by the square root of the diagonal elements of C

$$\Delta \widehat{\mathcal{C}}_b = \mathrm{C_{bb}^{1/2}}. \tag{15}$$

## 4. Results

Before we proceed to the study of the cross-correlation between the CMB polarization map and SXRB, we present an extensive analysis of the auto-correlation angular power spectrum of the two backgrounds revealed by ROSAT and WMAP, respectively. This allows us to have a better understanding of the statistical properties of our data sets.

We firstly work with the RSI maps in all the seven channels. Pixelizing the RSI sky under the angular resolution of 12' gives rise to a total pixels of $N_{\rm side} = 256$ in the HEALpix format. In order to match the WMAP angular resolution, the data are somewhat oversampled so that a value of $N_{\rm side} = 512$ is actually used, which has no influence on the construction of power spectra at large angular scales. We have tested a few of weighting functions to compensate for the incomplete sky coverage, and found that the results suffer from the contamination of foreground structures, such as the Galaxy and bright point sources in the soft X-ray band. We eventually use the R6 data within $b > 40^o$ and $l \in [70, 250]$, the so-called MSR mask, which is suggested as a better representative of the diffuse cosmological SXRB and less affected by the foreground structures (Śliwa et al. 2001). The angular power spectrum is constructed using the HEALPix package and the result is shown in Figure 1(a).

Next, we apply the same technique to the RSII map with pixel resolution $N_{\rm side} = 512$. Note that this sample has a wider energy coverage ranging from 0.2 to 2 keV. Since we make no attempt to edit the raw data except correct for the exposure time, the RSII map looks very noisy and a large fraction of the sky is apparently dominated by the emission of the Galaxy. We demonstrate the resulting angular power spectrum with mask MSR in Figure 1(b).

Despite the fact that the two samples have different energy coverages , the overall angular power spectra revealed by RSI and RSII maps are similar in shape. Two samples differ by several orders of magnitude in amplitude because the RSI maps divide up the flux of SXRB among seven energy bands ,and only the power spectrum of R6 band map is plotted in the Figure 1(a). The slight excess in the RSII power spectrum at large scales below $\ell \approx 100$ can be attributed to the emission from the galactic plane of the Galaxy. Furthermore, the two angular power spectra both have a steeper slope than $\ell(\ell+1)C_\ell \propto \ell^{0.8}$, indicating that the SXRBs are actually dominated by local sources (i.e., the Galaxy) rather than X-ray galaxies distributed at cosmological distances. Recall that the clustering of galaxies contributes an angular power spectrum of roughly $\ell(\ell+1)C_\ell \propto \ell^{0.8}$, provided that the sources follow a power-law angular power spectrum with an index of $\sim 0.8$ (Scott & White 1999). Yet, such a local component makes no contribution to the cross-correlation of SXRB and CMB polarization to be explored below.

Now we turn to the CMB polarization sky manifested by the Stokes Q and U parameters in the WP map. In a similar way to the analysis of the SXRB maps above, we apply two masks in the analysis of CMB polarization map; one is the full-sky WP data without any masks, and another is the so-called P06 mask used by the WMAP team (Page et al. 2007). For the latter, 25.7% of the sky is masked near the Galactic plane and around other strong sources of contamination, eliminating the effect of synchrotron polarization by the Galaxy, dust, point sources, etc. Indeed, the angular power spectra of polarization map with and without the P06 mask look rather different from each other, as illustrated in Figure 2 using the CMB TE cross-power spectrum. Apparently the structured power spectrum of the full-sky map originates from the foreground, and the structures vanish immediately when the contaminated regions of the sky are masked with the P06 mask. Shown also in the Figure 2 is the theoretically predicted CMB TE power spectrum calculated in terms of publicly available code CMBFAST[2]. It appears that the observationally measured and theoretically predicted power spectra agree each other nicely when the P06 mask is applied.

Finally we carry out the study of cross-correlation between the CMB polarization sky

[2]http://cfa-www.harvard.edu/ mzaldarr/CMBFAST/cmbfast.html

and SXRB using the ROSAT RSI and RSII samples and WP maps. Construction of cross-power spectra can be made straightforwardly, and the error bars of the cross-power spectra are estimated from 100 mock WMAP observational polarization maps and 100 mock SXRB maps using Eq. (14) and Eq. (15). The results of the cross-power spectra are shown in Figures 3 and 4 for RSI-WP and RSII-WP cross-correlations, respectively, for which we have considered the sky maps both with and without masks in order to demonstrate to what extent the angular power spectra are affected by the foreground sources. For the WP maps all the six polarization databases are employed and the results were averaged over the whole databases and the different observational band are illustrated, respectively. It turns out that, except for the RSII-WP cross-correlation without any masks, the rest are essentially consistent with the negative detection of cross-correlation between SXRB and CMB polarization maps. Recall that even in the full-sky coverage without the application of masks, such as MSR in the RSI (R6) sample, bright foreground X-ray sources have already been excised. Employment of the MSR allows one to further excise the Galactic disk from the samples. The absence of significant correlations between the RSI (with and without masks) or RSII (with mask MSR) samples and WP maps may therefore be of cosmological significance. We do detect a positive cross-correlation in the RSII-WP full-sky maps without any masks over angular scales of $\ell \approx 200 - 400$. Nevertheless, a careful examination of the RSII full-sky map shows that such a positive correlation is related to three strong X-ray emitting regions that are identified as Cyg Region, Gum Neb and Tau A in the WMAP point source catalog, which are strong X-ray source and supernova remnants. No correlation feature is detected once these three regions are excised or MSR and P06 masks are utilized (Figure 5). Actually, the result remains nearly unchanged if only one mask, either MSR or P06, is adopted to all the cases. The positive correlation associated with the three supernova remnants can be interpreted as the polarization of synchrotron in the regions or the polarization of CMB caused by the energetic electrons there, yielding the cross-correlation between X-ray emission and CMB polarization map.

## 5. Discussion and conclusions

The CMB polarization signals in large scale seen in the WMAP five-year data arise primarily from the scattering of free electrons in the epoch of reionization. At other scales, the primal quadrupole anisotropies are still dominant sources. But at small scales, the picture is more complicated. All types of the perturbations beyond linear order will contribute to the polarization signals. One possible source of polarization anisotropy at small scales is Thomson scattering by free electrons at the epoch of the reionization. Doré et al. (2007) find such polarization signals may have rms of order $\sim 0.01$ $\mu$K (see also Liu et al. 2001).

Other secondary contribution to the signals includes free electrons associated with large-scale structures through the warm-hot intergalactic medium (i.e. missing baryons) in local universe (Davé et al. 2001), and very energetic electrons in clusters of galaxies (Baumann & Cooray 2003) . These secondary effects ($\sim 10^{-4} - 10^{-5}\mu K$) are weaker than the polarization signals produced in the epoch of reionization and believed to be subdominant. Therefore, we focus on the possible reason for our negative detection of cross-correlation between ROSAT SXBR and WMAP CMB data. Indeed, there is good reason to believe that X-ray heating once playing a non-negligible contribution to the reionization of the universe. Primary sources of X-ray emission at high-redshift are high-mass X-ray binaries, supernovae and even QSOs. It is natural to expect a positive correlation between the CMB polarization and unresolved diffuse SXRB because both of them originate from the same epoch and follow the common underlying large-scale structures of the universe.

The most likely explanation for the negative detection of the cross-correlation between CMB polarization map and SXRB obtained with the WMAP and ROSAT maps may be due to the extremely faint signals that are buried in the strong foreground and instrumentation noise. Indeed, both CMB polarization and X-ray emission from the epoch of reionization are rather weak, and the latter has not even been separated from current SXRB. But if we assume that the CMB polarization signals due to the inhomogeneous process of the ionization of the universe (see Doré et al. 2007; Liu et al. 2001, for the estimation of such CMB polarization signals) were 100% correlated with the 5% of the soft X-ray emission which is emitted from high-redshift sources at the epoch of reionization, we can calculate this theoretical maximum correlations signals and take it as a rough estimate for the actual correlations signals. The results of the estimate, compared with the correlation results from the WMAP and ROSAT maps, are plotted as solid lines close to zero axes in Figure 3, 4, and 5. It is quit evident that even the theoretical maximum correlation signals are too weak to see in this measurement. Furthermore, if most of the CMB polarization is generated in the later time when the Ly$\alpha$ heating, instead of the X-ray heating, dominates the process of reionization, the strength of the cross-correlation between CMB polarization and SXRB would be even weaker. Therefore, a quantitative estimate of the cross-correlation and its measurement errors with existing and future instruments will be desired to explain our negative detection ultimately, and to forecast further prospects. The prime difficulty in carrying out such a theoretical investigation is the uncertainty of the effect of X-ray heating sources and their cosmic evolution in the epoch of reionization.

Obviously, such weak correlation signals will provide an ambitious target for upcoming experiments. Before a quantitative estimate is available, we can roughly evaluate the detectability of the correlation signals with the theoretical maximum signals estimate. Our

rough estimation of the noise cross-power spectra for Planck [3] ($\sigma = 2.3$ $\mu$K/5.0′ fwhm, 0.85% of the sky) and ACT (Atacama Cosmology Telescope; Kosowsky 2006) or SPTPol (South Pole Telescope; Ruhl et al. 2004) ($\sigma = 2.0$ $\mu$K/1.7′ fwhm, 0.25% of the sky) polarization data correlating with ROSAT RASS data are illustrated in Figure 6, respectively. The levels of the noise cross-power for CMB experiments like ACT or SPTPol are above the theoretical maximum signals levels, while those for Planck are under the theoretical maximum signal levels. It appears that such theoretical maximum signals might be detected with Planck at $\ell < 900$.

In summary, if X-ray heating is one of the major sources to ionize the neutral hydrogen in the epoch of reionization, we may expect to find a positive correlation between the unresolved diffuse SXRB and CMB polarization maps. Intuitively, our negative detection based on the ROSAT and WMAP data indicates that such a correlation is rather weak, and experiments with higher sensitivities are required to make further explorations. Yet, our negative result can be used to constrain the theory of X-ray heating in the epoch of reionization. From our result, the theoretical prediction of the cross power spectra between R6 band SXRB and CMB polarization could not be out of range $-0.8 \lesssim \ell(\ell+1)/2\pi\ C_\ell \lesssim 0.7$ (mK $10^{-6}$cts/s/arcmin$^2$) at $\ell \simeq 300$, $-1.5 \lesssim \ell(\ell+1)/2\pi\ C_\ell \lesssim 1.2$ at $\ell \simeq 500$, $-3.3 \lesssim \ell(\ell+1)/2\pi\ C_\ell \lesssim 3.2$ at $\ell \simeq 800$ (based on the result from RSI R6 band map and WP maps). And those between wider energy band (0.2 KeV $\sim$ 2 KeV) SXRB and CMB polarization could not be out of range $-3.3 \lesssim \ell(\ell+1)/2\pi\, C_\ell \lesssim 3.2$ (mK $10^{-6}$cts/s/arcmin$^2$) at $\ell \simeq 300$, $-9.7 \lesssim \ell(\ell+1)/2\pi\, C_\ell \lesssim 7.0$ at $\ell \simeq 500$, $-36.4 \lesssim \ell(\ell+1)/2\pi\ C_\ell \lesssim 30.2$ at $\ell \simeq 800$ (based on the result from RSII map and WP maps). Meanwhile, a detailed study of the cross power spectrum would be is also worthy to guide future observations.

We thank theWMAPand ROSAT teams for making their data available via the Legacy Archive for Microwave Data Analysis (LAMBDA) at http://lambda.gsfc.nasa.gov and the ROSAT XRay All-Sky Survey archive at http://www.xray.mpe.mpg.de/ cgi-bin/rosat/rosat-survey. This work was supported by the National Science Foundation of China (Grant no. 10673008) and the NCET Program of Ministry of Education, China.

## REFERENCES

Afshordi, N., Loh., Y. S., & Strauss, M. A. 2004, Phys. Rev. D, 69, 083524

Banday, A. J., et al. 1996, ApJ, 468, L85

[3]http://www.rssd.esa.int/Planck

Baumann, D., & Cooray, A. 2003, New Astronomy Review, 47, 839

Bennett, C. L., et al. 1993, ApJ, 414, L77

Bennett, C. L., et al. 2003, ApJ, 583, 1

Boughn, S. P., & Jahoda, K. 1993, ApJ, 412, L1

Boughn, S. & Crittenden, R. 2004a, Nature, 427. 45

Boughn, S. & Crittenden, R. 2004b, ApJ, 612, 647

Brown, M. L., Castro, P. L., & Taylor, A. N. 2005, MNRAS, 360, 1262

Bryan, G. L., & Voit, G. M. 2001, ApJ, 556, 590

Challinor, A. D., & Chon, G. 2005, MNRAS, 360, 509

Chen, X., & Miralda-Escudé, J. 2004, ApJ, 602, 1

Cooray, A., & Baumann, D. 2003, Phys. Rev. D, 67, 063505

Davé, R., et al. 2001, ApJ, 552,473

Diego, J. M., Silk, J., & Silwa, W. 2003, MNRAS, 346, 940

Dijkstra, M., Haiman, z., & Loeb, A. 2004, ApJ, 613, 646

Doré, O., Holder, G., Alvarez, M., Iliev, I. T., Mellema, G., Pen, U.-L., & Shapiro, P. R. 2007, Phys. Rev. D, 76, 043002

Fosalba, P., & Gaztanaga, E. 2004, MNRAS, 350, L37

Hansen, F. K., & Górski, K. M. 2003, MNRAS, 343, 559

Hinshaw, G., et al. 2007, ApJS, 170, 228

Hivon, E. et al. 2002, ApJ, 567, 2

Kneissl, R., et al. 1997, A&A, 320, 685

Kogut, A., et al. 2007, ApJS, 665, 355

Kosowsky, A. 2006, New Astronomy Review, 50, 969

Lewis A., Challinor A., & Turok N., 2002, Phys. Rev. D, 65, 023505

Liu, G.-C., Sugiyama, N., Benson, A. J., Lacey, C. G., & Nusser, A. 2001, ApJ, 561, 504

Moretti, A., et al. 2003, ApJ, 588, 696

Myers, A. D., Shanks, T., Outram, P. J. & Wolfendale, A. W. 2004, MNRAS, 347, L67

Nolta, M. R., et al. 2004, ApJ, 608, 10

Page, L., et al. 2007, ApJS, 170, 335

Pietrobon, D., Balbi, A., & Marinucci, D. 2006, Arxiv Astrophysics e-prints, arXiv:astro-ph/0611797

Ruhl, J., et al. 2004, Proc. SPIE, 5498, 11

Salvaterra, R., Haardt, F. 2007, MNRAS, 374, 761

Scott, D., & White, M. 1999, A&A, 346, 1

Scranton, R. et al. 2003, Arxiv Astrophysics e-prints, arXiv:astro-ph/0307335

Shimon, M., Rephaeli, Y., O'Shea, B. W., & Norman, M. L. 2006, MNRAS, 368, 511

Snowden, S. L., et al. 1997, ApJ, 485, 125

Śliwa, W., Soltan, A. M., & Freyberg, M. J. 2001, A&A, 390, 397 & Volonteri, M. 2007, MNRAS, 374, 761

Weller, J. 1999, ApJ, 527, L1

Wu, X.-P., & Xue, Y.-J. 2001, ApJ, 560,544

Wu, X.-P., & Xue, Y.-J. 2003, ApJ, 590, 8

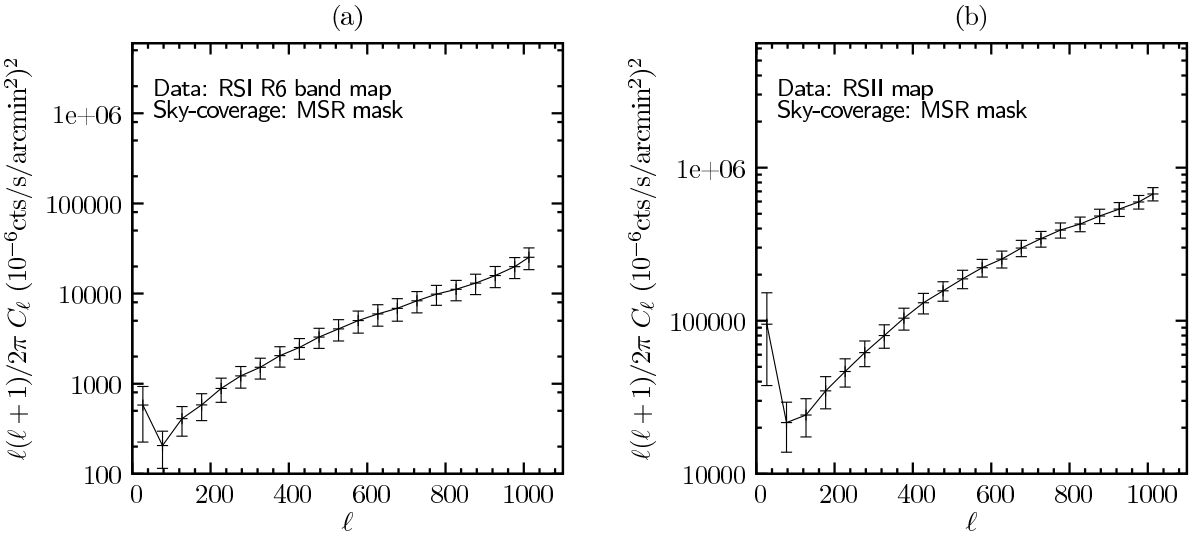


Fig. 1.— Angular power spectra revealed by the RSI and RSII samples. The $1\sigma$ error bars are estimated using the WMAP simulations. Both angular power spectra are binned in terms of $\Delta\ell = 30$

.

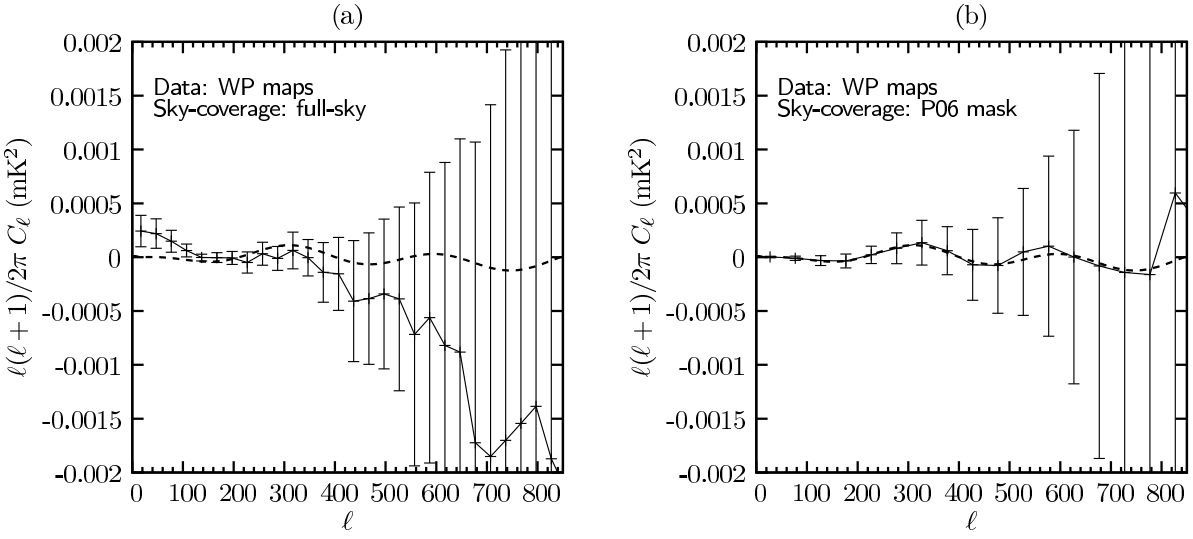


Fig. 2.— TE angular power spectra constructed from WP maps(V1, V2, W1, W2, W3, W4 data) with (b) and without (a) P06 mask, respectively. The solid lines represent the results obtained with the WP maps and the dashed lines are the theoretically predicted power spectrum generated by CMBFAST. The angular power spectrum constructed from the maps with masks are binned in terms of $\Delta\ell = 50$.

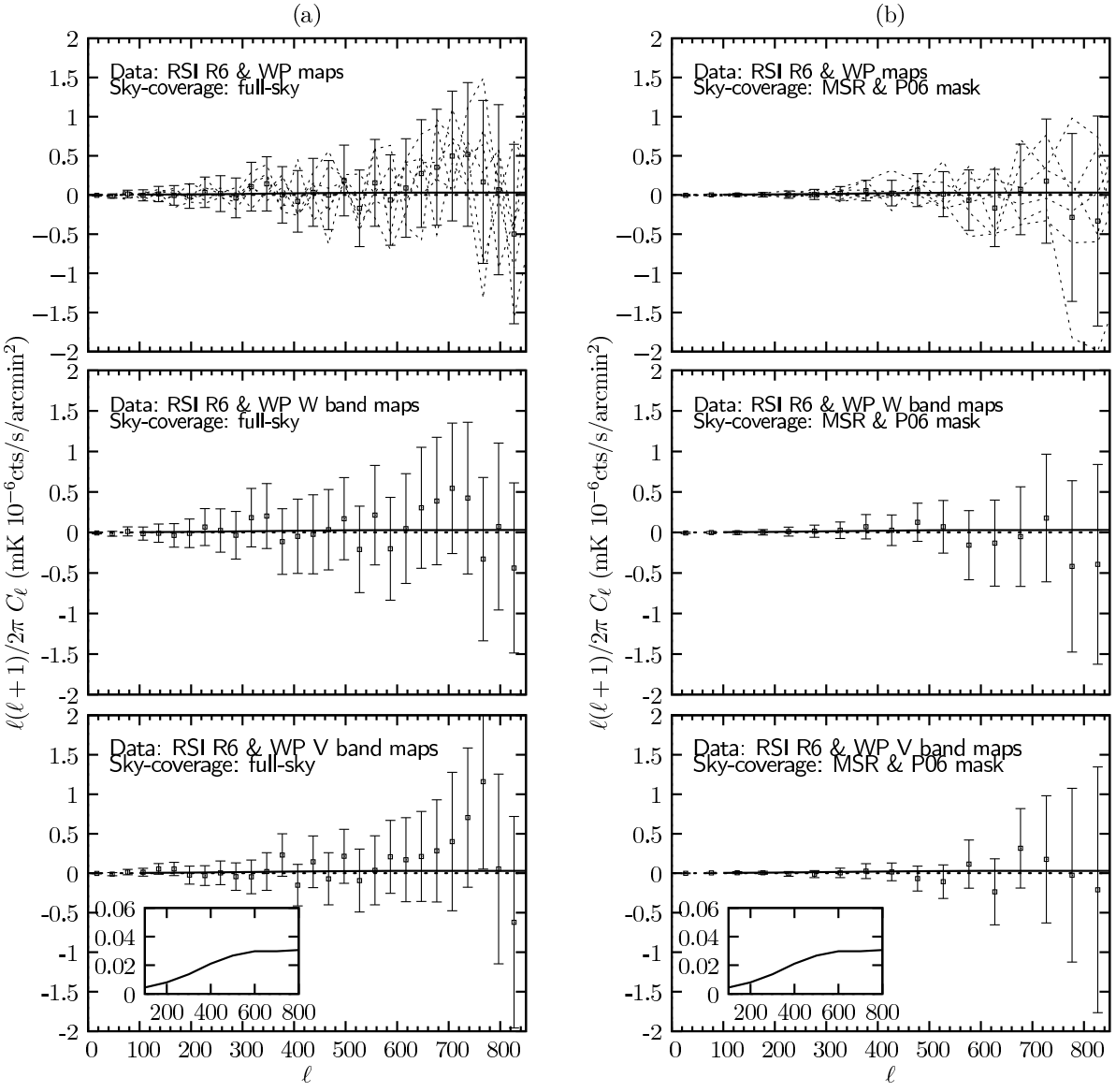


Fig. 3.— Cross-power spectra constructed from RSI R6 sample and WP six databases (dotted lines), and the open squares with error bars represent their averages over the whole database ( top panel ), V ( middle panel ), and W ( bottom panel ) band. The solid line close to the zero axis represents the estimate of maximum correlation signals (see Section 5 for details). The small graph sketches the estimate correlations signals with magnifying Y-range.

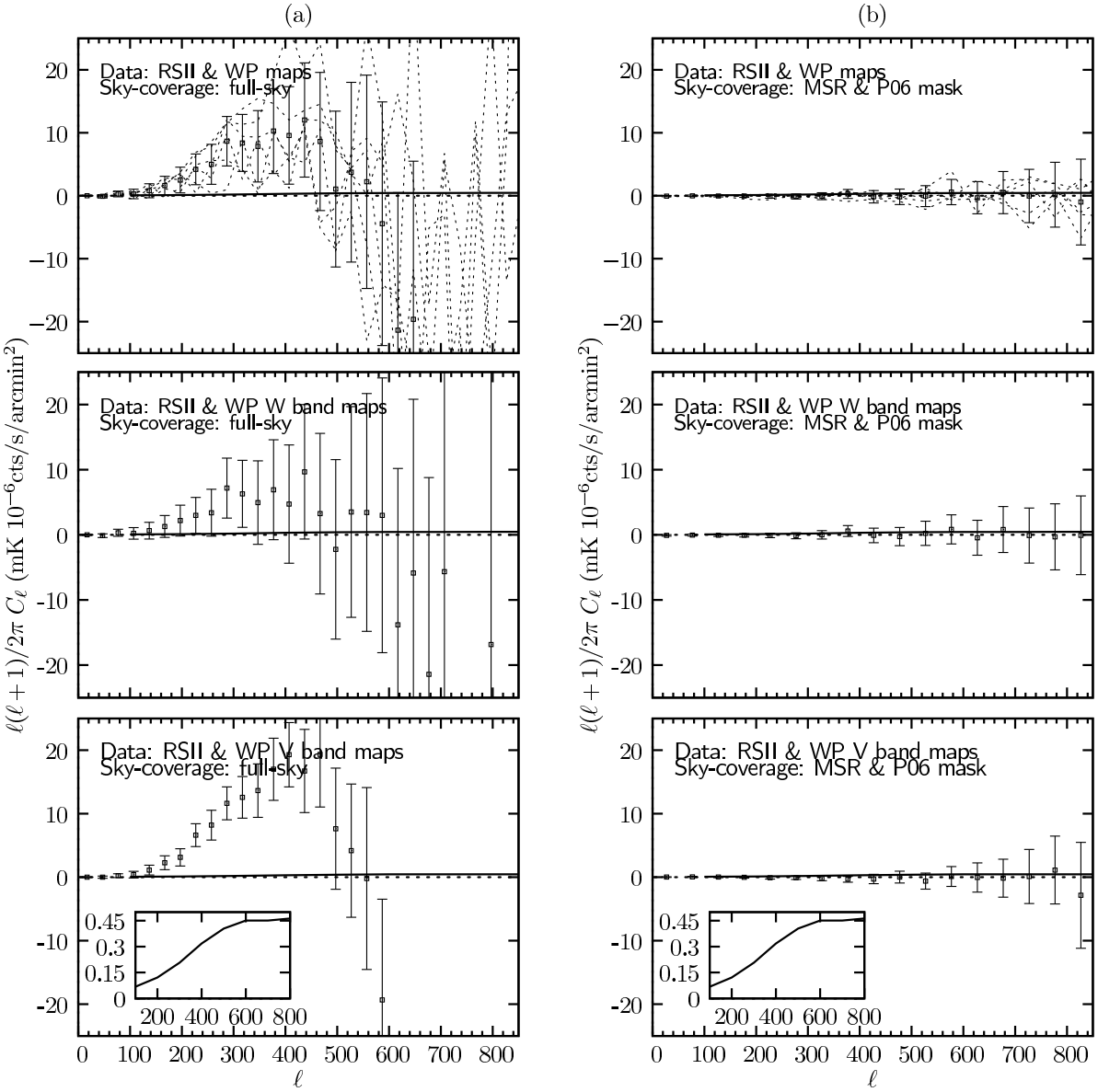


Fig. 4.— Same as Figure 3, but for RSII sample.

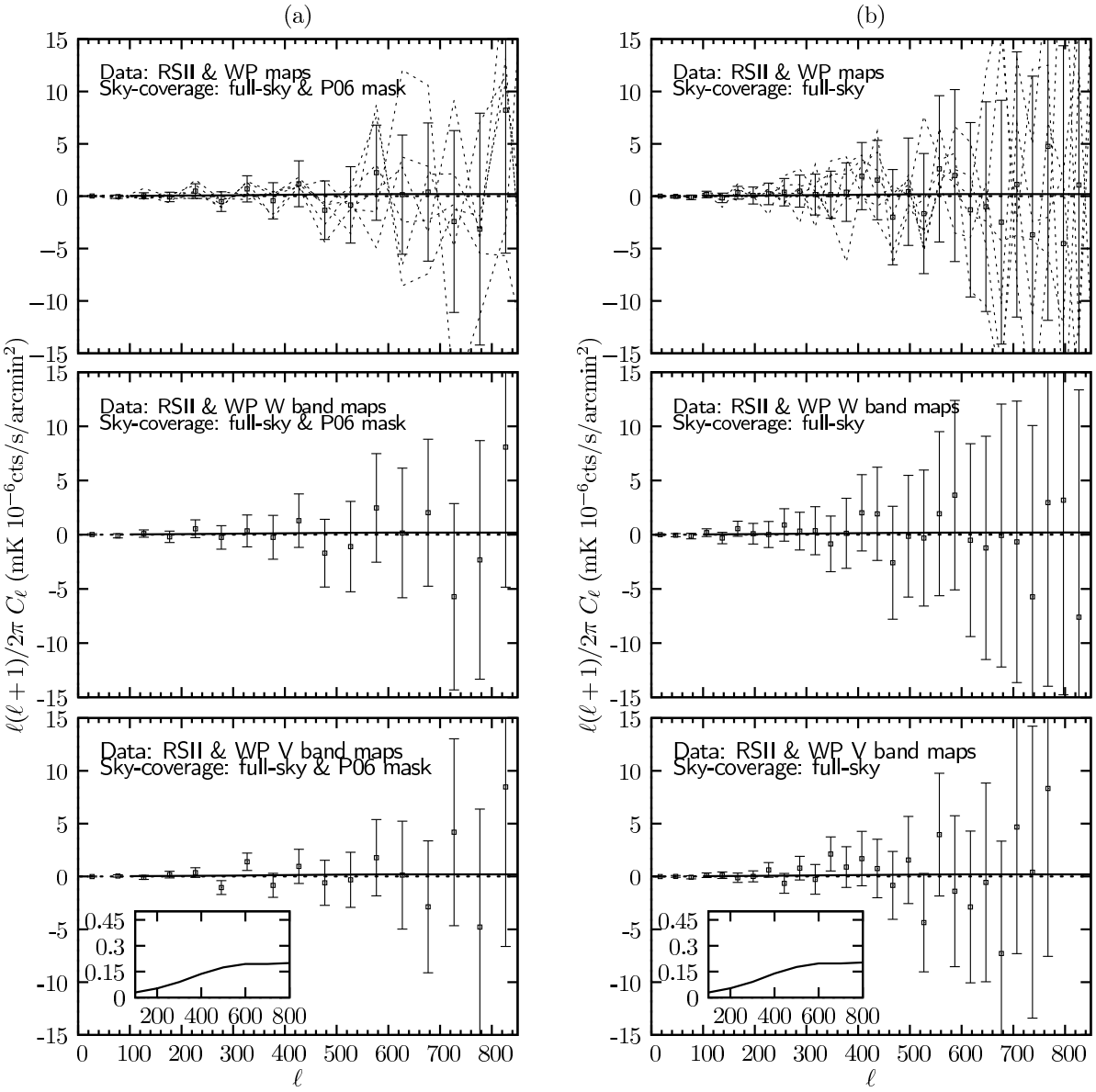


Fig. 5.— Same as Figure 3, but for the full-sky RSII sample with (a) the P06 mask on WP maps and (b) removal of three bright X-ray sources in Galactic plane (Cyg Region, Gum Neb and Tau A).

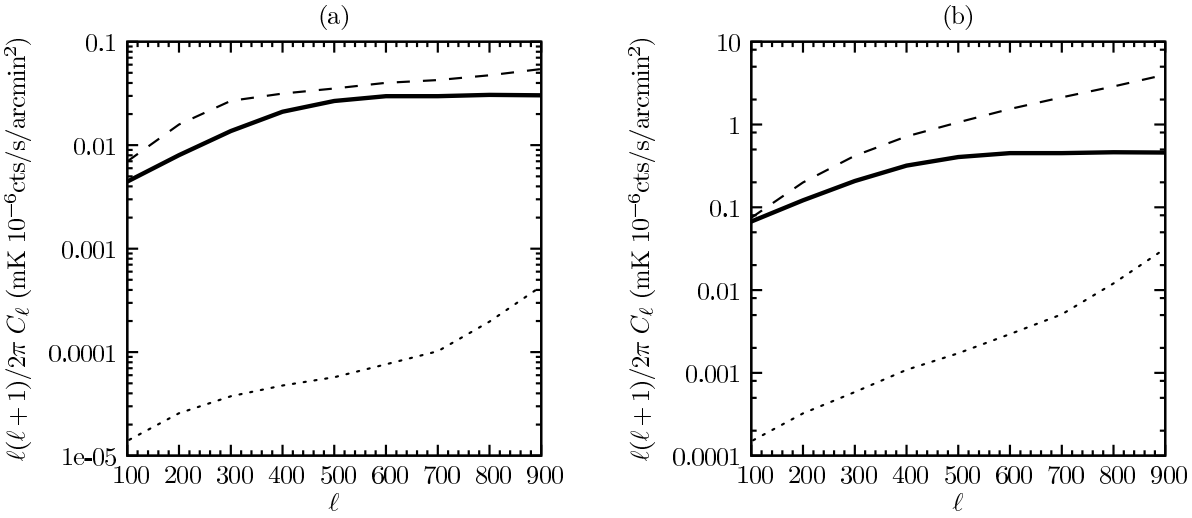


Fig. 6.— Theoretical maximum correlation signals one could expect compares with the estimated noise of the cross-power spectrum for the upcoming experiments. The heavy solid lines represent the estimated maximum signals from CMB polarization map correlating with RSI R6 band map (a) and RSII map (b), respectively. The estimation of the noise cross-power spectrum for Planck polarization and SXRB maps is shown as dotted lines, while the estimation for the polarization observation like ACT or SPTPol and SXRB maps is shown as dash lines.